27th IECEC, Society of Automotive Engineers
1992, pp. 3.493-3.497

Phase Diagram and Electrical Behavior of Silicon-rich Iridium Silicide Compounds

C. E. Allevato and Cronin B. Vining
Jet Propulsion Laboratory/California Institute of Technology Pasadena, California 91109

ABSTRACT

The iridium-silicon phase diagram on the silicon-rich side was investigated by means of X-ray powder diffraction, density, differential thermal analysis, metalography, microprobe analysis, and electrical resistivity. Attempts were made to prepare eight previously reported silicon-rich iridium silicide compounds by arc melting and Bridgman-like growth. However, microprobe analysis identified only four distinct compositions: IrSi, Ir_3Si_4, Ir_3Si_5 and $IrSi_{\sim 3}$. The existence of Ir_4Si_5 could not be confirmed in this study, even though the crystal structure has been previously reported. Differential thermal analysis (DTA) in conjunction with X-ray powder diffraction confirm polymorphism in $IrSi_{\sim 3}$, determined to have orthorhombic and monoclinic unit cells in the high and low temperature forms. A eutectic composition alloy of 83±1 atomic % silicon was observed between $IrSi_{\sim 3}$ and silicon. Ir_3Si_4 exhibits distinct metallic behavior while Ir_3Si_5 is semiconducting. Both and IrSi and $IrSi_{\sim 3}$ exhibit nearly temperature independent electrical resistivities on the order of $5\text{-}10 \times 10^{-6}$ Ω-m.

INTRODUCTION

The transition metal silicides form a series of refractory compounds[1] ranging in chemical bonding from metallic to covalent, suggesting a great variety of interesting physical properties. Some of these compounds may be of particular interest for thermoelectric space power applications since the high mass of iridium favors low thermal conductivity values and high melting points allow high heat rejection temperatures, both of which are advantages for efficient thermoelectric power devices.[2] Unfortunately, the phase diagram has not yet been determined and most of the work involving iridium silicides deal with non-equilibrium thin films. The current study focused on silicon-rich materials in order to identify which, if any, of the compounds in the Ir-Si system might be of interest for thermoelectric applications.

According to Finnie,[3] the Ir-Si system is mostly in the solid state at 1610 K and seven phases could be identified by X-ray diffraction.[4] Nicolet and Lau[5] describe more than 8 intermediate phases. More recent investigations by Petersson[6] and Wittmer[7] of the interaction of iridium films with silicon substrates revealed the existence of only 3 distinct phases: 1) IrSi observed between 673 and 873 K; 2) a phase with composition close to Ir_4Si_7 observed from 773 K to 1223 K; and 3) $IrSi_{\sim 3}$ observed at temperatures in the vicinity of 1273 K.

Petersson,[8] Bost[9] and Frampton[10] suggest that the compound identified as Ir_4Si_7 is a semiconductor. Engström,[11] determined the correct composition of this compound as Ir_3Si_5 by single crystal X-ray diffraction studies.

In contrast to the semiconducting behavior in Ir_3Si_5, White[12] and Bhan[13] report that iridium trisilicide, $IrSi_{\sim 3}$, has a metal-like resistivity and a hexagonal crystal structure. Engström and Zdansky[14] investigated polycrystalline, arc melted $IrSi_{\sim 3}$ and found an orthorhombic crystal structure which, after heat treatment for one week at 1173 K, transformed to a monoclinic form. Subsequent heat treatment at 1273 K reversed the phase transition. The reported metal-like behavior of $IrSi_{\sim 3}$ is surprising considering the unusually high silicon content of this compound.

The existence of other compounds such as Ir_4Si_5 (ref. 15), Ir_2Si_3 (ref. 6, 15 and 16) and even $IrSi_2$ (ref. 17, 18, and 19) have been suggested, but nothing is known concerning their transport behavior. The rule of 14 valence electrons per metal discussed by Jeitschko,[20] predicts that the composition Ir_4Si_5 should be a semiconductor. Although the structure reported for Ir_4Si_5 (ref. 15) is distinct from the structure class discussed by Jeitschko, valence electron counting nevertheless suggests that one or more of the silicon-rich iridium silicides might be semiconducting.

EXPERIMENTAL DETAILS

The aim of this investigation is to verify the existence of eight Si-rich iridium silicide compounds previously noted in the open literature. Samples were prepared by arc-melting on a water cooled copper hearth and using a two zone graphite heating element furnace with pyrolytic boron nitride crucibles.

Arc melted samples were prepared from high purity (99.95%) iridium powder with a -60 mesh, premelted into beads of approximately 4 grams each. Silicon was obtained from single crystal wafers cut into small pieces of different sizes and shapes. Specimens were produced by melting

stoichiometric amounts of pure iridium and silicon and were remelted 2-3 times in an argon filled arc-furnace. The following nominal compositions were prepared with weight losses less than 0.9%.: IrSi, Ir_4Si_5, Ir_3Si_4, Ir_2Si_3, Ir_3Si_5, Ir_4Si_7, $IrSi_2$ and $IrSi_{\sim3}$. Compositions identified in the arc melted samples were afterward prepared by Bridgman-like growth under 2 psi He pressure. One compound with 57 at% Si was obtained by quenching from the melt in a boron nitride crucible.

Samples were mounted, polished and examined under an optical phase contrast microscope. Microprobe analysis were determined with a Jeol superprobe using the Ir L line, the Si K line at 20 keV. Results were calculated by the Caltech ZAF program. The compound Ir_3Si_5 was used as a standard with an accuracy greater than ±1% for the specific elements of iridium and silicon. A study of the amount of different phases in each sample was acquired by using a Kevex Delta Energy Dispersive Analyzer of X-Rays in conjunction with feature analysis.

The critical temperature of each sample was determined by differential thermal analysis (DTA) in a DuPont 1600 °C DTA furnace using pyrolytic boron nitride crucibles and argon as the purge gas. The boron nitride crucibles delaminated during cycling but otherwise functioned satisfactorily and were non-reactive with the samples. The heating rate was 25 K/minute up to 1123 K and 10 K/minute to a temperature greater than the melting point, except for the IrSi sample which had a melting point higher than the upper limit of the DTA furnace of 1873 K. The DTA, calibrated using pure gold and silicon samples as standards, has an estimated uncertainty of about ±5 K.

The melting point of four samples were also determined by an independent method using the same two-zone furnace used for sample growth, but in this case the temperature profile nearly uniform. Furnace control temperatures, determined by optical pyrometry, were calibrated using W-5%Re/W-26%Re thermocouples and by melting high purity standards of elemental Si, Ge and Pt. Only small corrections (±15 K) were required. Iridium silicide samples were heated in boron nitride crucibles under He gas, cooled to room temperature and examined visually. If the sample had not melted, the procedure was repeated at a higher temperature until the entire sample had melted. Melting points determined by this method were in agreement with DTA results to within 15 K for three samples determined by both methods.

Density measurements were performed in toluene by the Archimedes method and all density values were repeatable to within 0.5%. A Siemens D-500 diffractometer Cu-K_α radiation was used to obtain powder X-ray patterns with a step scan interval of 2Θ=0.05 degree and a 7 second count time. Electrical resistivity measurements were performed by means of the van der Pauw[21] method from 300 to 1330 K, neglecting any anisotropy effects.

RESULTS AND DISCUSSION

Results obtained with the above techniques are summarized in Table 1 and in the phase diagram of Figure 1. Four distinct phases were observed to form in quantities detectable by microprobe analysis. In the following section, we discuss the various results in more detail.

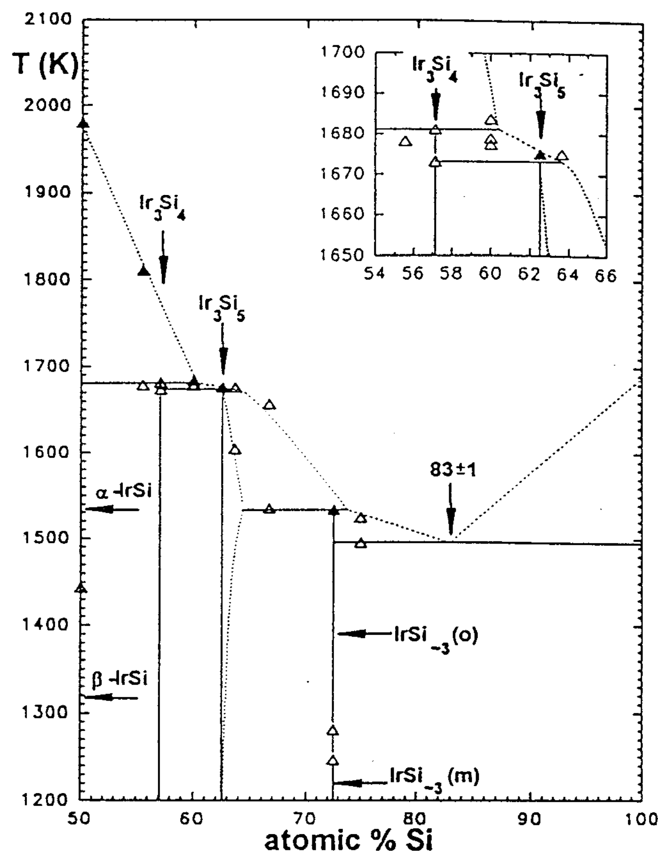

Figure 1. Silicon-rich iridium silicon phase diagram. (△) determined by DTA, (▲) determined by DTA and direct observation (except for the IrSi melting point which was beyond the range of the DTA equipment).

IrSi

Single phase iridium monosilicide was obtained by arc melting stoichiometric amounts of the elements and also by Bridgman growth with an initial composition corresponding to Ir_4Si_5. Typically, IrSi grains exhibit striation-like defects clearly visible in optical micrographs. Microprobe analysis of the arc melted sample showed only trace amounts of Ir_2Si (less than 1%). Several attempts to grow crack free IrSi by the Bridgman method were unsuccessful. IrSi obtained by arc melting had an X-ray powder diffraction pattern and density consistent with catalog data[22] corresponding to the orthorhombic form, refereed to here as α-IrSi. However, the IrSi obtained by the Bridgman method showed slight shifts and splitting of several X-ray lines (shown in Figure 2) and a distinctly lower density, indicating a modification (possibly monoclinic) of the orthorhombic structure, refereed to here as β-IrSi.

Table 1. Observed intermediate phases in the silicon-rich portion of the iridium silicide compounds.

Phase	Structure Type	Ref.	Composition atomic % Si	Density (g/cm^3) Calc.	Density (g/cm^3) Exp. (±0.5%)	Critical Temperature (K) DTA (±5K)	Critical Temperature (K) Other* (±10K)	Resistivity 10^{-8} Ω-m
α-IrSi	MnP	(15)	50.1±0.5	13.00	12.51		1980	500
β-IrSi	Distorted-MnP	(this work)	50.1±0.5	-	11.56	1443		-
Ir_3Si_4	Rh_3Si_4	(15)	57.0±0.6	11.36	10.89	1681		60
Ir_3Si_5	Ir_3Si_5	(11)	62.5±0.6	10.17	10.12	1675	1688	200000
$IrSi_{\sim3}$(o)	orthorhombic	(14)	72.5±0.7	8.44	8.21	1533	1528	350
$IrSi_{\sim3}$(m)	monoclinic	(14)	-	8.43	-	1274		580

*Determined by visual observation as described above.

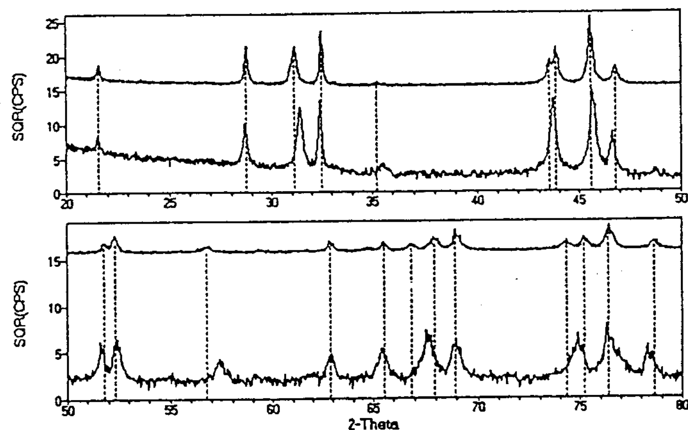

Figure 2. X-ray diffraction of pattern of orthorhombic α-IrSi (upper curve, prepared by arc melting) compared to β-IrSi (lower curve, prepared by Bridgman growth).

Differential thermal analysis carried out up to 1673 K showed a significant transition at 1443 K. This might be an indication that the modified form prevails below this temperature. The melting point of 1980 K for IrSi was obtained by the visual observation method described above.

The electrical resistivity of α-IrSi, shown in Figure 3, is only weakly temperature dependent. The resistivity increases from 4.5×10^{-6} Ω-m at 300 K to a maximum of 5.6×10^{-6} Ω-m at 950 K, after which the resistivity decreases to 5.1×10^{-6} Ω-m at 1300 K.

Ir_3Si_4

Microprobe analysis identified only one phase between IrSi (50% Si) and Ir_3Si_5 (62.5% Si). The density, composition determined by microprobe (57.0% ± 0.5% Si) and the X-ray powder diffraction pattern are in excellent agreement with the Ir_3Si_4 compound reported by Engström.[15] Neither microprobe nor X-ray diffraction yielded any evidence for the compound Ir_4Si_5 (55.6% Si), also reported by Engström.[15]

Arc melted samples with nominal compositions Ir_4Si_5, Ir_3Si_4 and Ir_2Si_3 exhibit a dendritic microstructure, becoming less dense with increasing silicon content, as shown in Figure 4. Typical eutectic microstructures were not observed in this composition range. Microprobe analysis indicate the dendrite core to be IrSi surrounded by Ir_3Si_4 in a Ir_3Si_5 matrix. Attempts to obtain a sample with a composition of Ir_4Si_5 by Bridgman growth lead to the monosilicide as stated above. The electrical resistivity of the Ir_3Si_4 compound was 6×10^{-7} Ω-m at 300 K and exhibited an increase with increasing temperature (Figure 3), typical of metals.

Ir_3Si_5

Single phase, polycrystalline Ir_3Si_5 was prepared by arc melting with density and X-ray patterns in good agreement with the monoclinic structure reported by Engström.[11] Initial attempts to grow this compound by the Bridgman method from a stoichiometric melt were not successful, although growth from a slightly Si-rich melt may be possible. The Ir_3Si_5 sample prepared by arc melting forms at 1675 K and

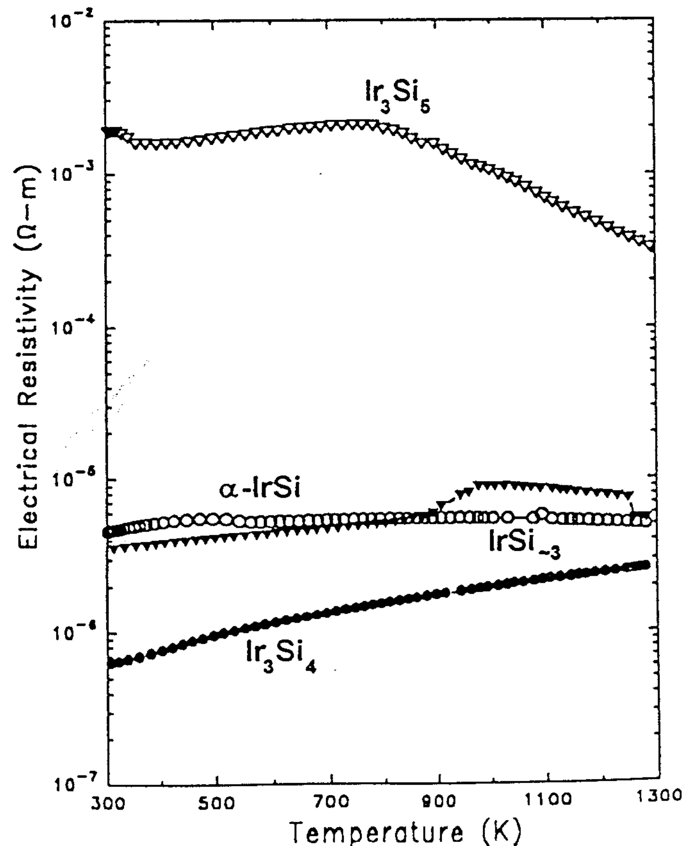

Figure 3. Electrical resistivity as a function of temperature for four iridium silicides.

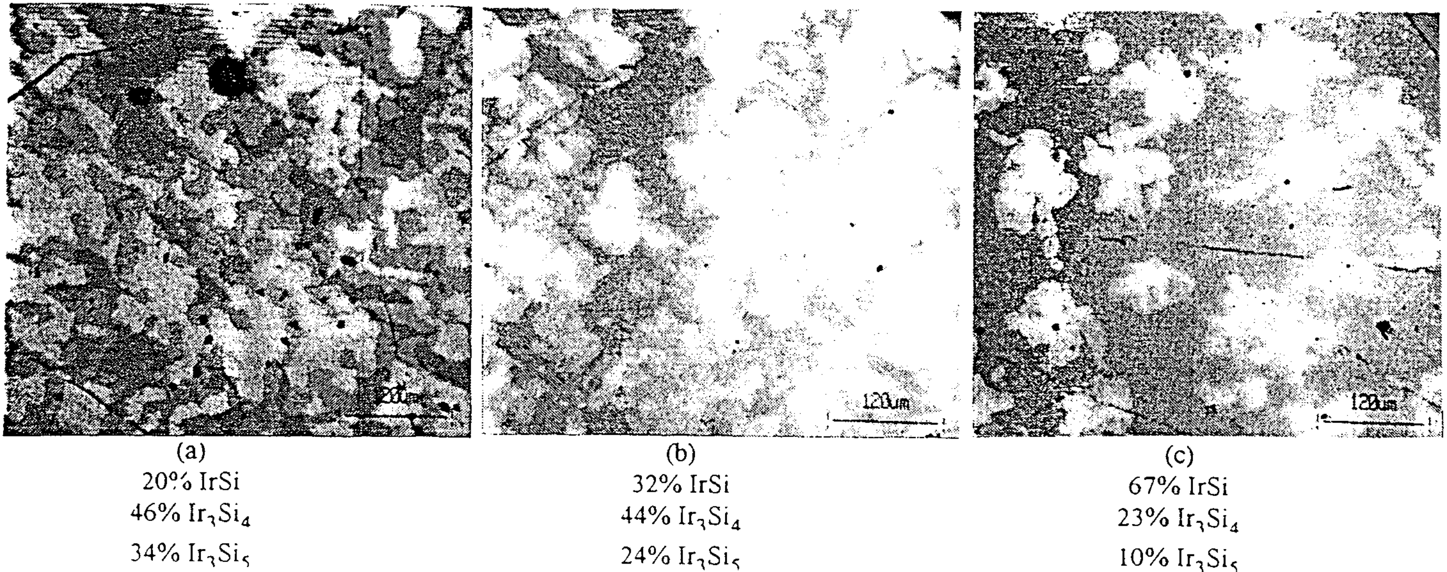

(a)	(b)	(c)
20% IrSi	32% IrSi	67% IrSi
46% Ir_3Si_4	44% Ir_3Si_4	23% Ir_3Si_4
34% Ir_3Si_5	24% Ir_3Si_5	10% Ir_3Si_5

Figure 4. Micrographs showing dendrites observed in arc melted samples with different nominal compositions: (a) Ir_4Si_5, (b) Ir_3Si_4, and (c) Ir_2Si_3

showed no trace of any eutectic alloy.

Differential thermal analysis of a sample with nominal composition of Ir_4Si_7 revealed two major transitions at 1675 K and at 1604 K. This result suggests a homogeneity range which depends on temperature for the compound Ir_3Si_5 as indicated in the phase diagram (Figure 1). The compound Ir_3Si_5 shows a resistivity profile (Figure 3) that resembles the behavior of a semiconductor and Hall effect measurements indicate the sample is p-type over the entire temperature range. The resistivity at room temperature is 2×10^{-3} Ω-m and decreases to 2×10^{-4} Ω-m at 1300 K, which is relatively high to be considered as a metal.

$IrSi_{\sim3}$

Slightly higher weight losses, around 1.3%, resulted when arc melting $IrSi_{\sim3}$ compared to less Si-rich compositions. A eutectic structure consisting of $IrSi_{\sim3}$ and pure silicon was observed by microprobe analysis with a composition of 83±1% Si, as shown in Figure 5.

Figure 5. Eutectic composition alloy showing the intimate mixture of $IrSi_{\sim3}$ (light) and Si (dark).

A single phase sample of $IrSi_{\sim3}$ was obtained by the Bridgman technique, with evidence of a eutectic alloy only at the top of the ingot. DTA and visual observation of a single phase portion of this sample indicate melting at about 1533 K. DTA also showed evidence of small transitions at 1247 K and 1281 K, consistent with the existence of polymorphism as suggested by Engström.[14]

X-ray powder diffraction on the as-prepared Bridgman grown sample of $IrSi_{\sim3}$ agreed reasonably well with the pattern reported by Engström[14] for the orthorhombic form, $IrSi_{\sim3}$(o), although a few additional peaks were observed. Engström[14] suggests the true stoichiometry corresponds to a composition of 74% Si. Microprobe analysis performed in the present work on this phase leads to the value of 72.5± 0.7% Si, which again is slightly less than the ideal trisilicide composition. The experimental density of 8.20 g/cm^3 is in close agreement with the theoretical density of 8.48 g/cm^3 indicated by Finnie,[3] as well as with an experimental value 8.64 g/cm^3 reported by Bhan and Schubert.[13]

Electrical resistivity measurements performed on Bridgman grown $IrSi_{\sim3}$, shown in Figure 3, indicate two relatively sharp features. The resistivity slowly increases with increasing temperature. Between 900 K and 1000 K the resistivity increases rapidly to a maximum of 8.9×10^{-6} Ω-m at about 1000 K. Then, the resistivity slowly decreases with further increase in temperature and at 1265 K the resistivity suddenly drops by about 35% to 5.5×10^{-6} Ω-m. The sudden change in resistivity observed at 1265 K is presumed to be related to similar features observed by DTA at 1274 and 1281 K.

Upon cooling, the resistivity exhibited significant hysteresis (not shown) and returned to a room temperature resistivity value of 5.8×10^{-6} Ω-m, significantly above the room temperature value of 3.5×10^{-6} Ω-m observed in the as-prepared state. The X-ray diffraction pattern also changed after thermal cycling and agreed quite well with the

monoclinic $IrSi_{\sim3}$(m) pattern reported by Engström.[14] No features were observed by DTA performed on this sample.

$IrSi_{\sim3}$(o) has been observed only in as-prepared samples, both in this study and by Engström.[14] Presumably this is the high temperature form and $IrSi_{\sim3}$(m) is the stable low temperature form. At the beginning of the resistivity measurements, the Bridgman grown $IrSi_{\sim3}$ sample was frozen in the orthorhombic form. The rapid increase in resistivity between 900 and 1000 K may represent transformation to the more stable monoclinic form. Similarly, the sharp decrease in resistivity at about 1265 K may represent return of the sample to the orthorhombic form, which appears to be the stable form above this temperature.

CONCLUSION

The present investigation allowed for the first time determination of the Ir-Si phase diagram on the Si-rich side. IrSi appears to be polymorphic, exhibiting either the previously reported[22] orthorhombic unit cell (α-IrSi) or a closely related, possibly monoclinic unit cell (β-IrSi). DTA suggests the β-form is the stable structure below 1443 K. The monosilicide melts at 1980 K, presumably congruently, and shows metallic conduction.

The existence of Ir_3Si_4 was confirmed with a peritectic formation temperature of 1681 K. This compound exhibits metallic conduction. The existence of Ir_4Si_5, however, could not be confirmed. Possibly Ir_4Si_5 forms by solid state reaction, similar to the peritectoidal formation of Rh_4Si_5 (ref. 23), and could be prepared by appropriate annealing.

A peritectic formation temperature of 1675 K was determined for Ir_3Si_5 and the semiconducting behavior of this compound was confirmed. While the precise melting behavior requires further study, Ir_3Si_5 appears to occur over a range of compositions at high temperatures.

The most silicon-rich compound in the Ir-Si system, indicated as $IrSi_{\sim3}$, has a composition of about 72.5% Si, a peritectic decomposition temperature of 1533 K and transforms from a high temperature orthorhombic structure to a low temperature monoclinic structure at about 1274 K. Both forms exhibit semi-metallic or heavily doped semiconducting behavior.

Several features of the Ir-Si phase diagram require further study, such as the polymorphism observed in IrSi and $IrSi_{\sim3}$ as well as the high temperature homogeneity range of Ir_3Si_5. Also, the Ir-rich side of the Ir-Si system remains to be determined. The two most silicon-rich compounds, Ir_3Si_5 and $IrSi_{\sim3}$, appear to be p-type and may be of interest for thermoelectric applications.

ACKNOWLEDGEMENTS

The work described in this paper was carried out at the Jet Propulsion Laboratory, California Institute of Technology, under contract with the National Aeronautics and Space Administration. The authors wish to express their gratitude to Prof. B.T. Fultz of the California Institute of Technology for providing access to arc melting facilities, P. Carpenter for the microprobe analysis, to L. Lowry and J. Kulleck for the X-ray pattern, R. Ruiz for EDX, J. McCormack for the Hall effect measurements, and G. Hickey for the DTA.

REFERENCES

1. K.N. Mason, *Prog. Crystal Growth Charact.* **2**, 269 (1979).
2. A.W. Searcy, D.J. Mesch in ***Thermoelectricity***, edited by P.H. Egli (Wiley and Sons, New York/London), 159 (1960).
3. L.N. Finnie, *J. Less-Common Metals* **4,** 24 (1962).
4. K. Schubert, S. Bhan, W. Burkhardt, R. Gohle, H.G. Meissner, M. Potzschke, E. Stoltz, *Naturwiss*, **47**, 303 (1960).
5. M.A. Nicolet and S.S. Lau in ***VLSI Electronics: Microstructure Sciences***, Vol. 6, edited by N.G. Einspruch and G.B. Larrabee, (Academic Press, New York) 329 (1983).
6. S. Petersson, J. Baglin, W. Hammer, F. d'Heurle, T.S. Kuan, I. Ohdomary, J. de Souza Pires, and P. Tove, *J. Appl. Phys.* 50(5), 3357 (1978).
7. M. Wittmer, P. Oelhafen, K.N. Tu, *Phys. Rev.* **B35**(17), 9073 (1987).
8. S. Petersson, J.A. Reimer, M.H. Brodsky, D.K. Campbell, F. d'Heurle, B. Karlsson, and P.A. Tove, *J. Appl. Phys.* 53(4), 3342 (1982).
9. M.C. Bost, J.E. Mahan, *J. Vac. Sci. Technol.* **B4**(6), 1336 (1986).
10. R.D. Frampton and E.A. Irene, *J. Appl. Phys.* **59**(3), 978 (1986).
11. I. Engström, T. Sindsten, and E. Zdansky, *Acta Chem. Scand.* **A41**, 237 (1987).
12. J.G. White, E.F. Hockings, *Inorg. Chem.* **10**(9), 1934 (1971).
13. S. Bhan and K. Schubert, *Z. Metallkde* **51**, 327 (1960).
14. I. Engström and E. Zdansky, *Acta Chem. Scand.* **A36**(10), 857 (1982).
15. I. Engström and F. Zackrisson, *Acta Chem. Scand.* **24**, 2109 (1970).
16. I. Ohdomari, T.S. Kuan, K.N. Tu, *J. Appl Phys.* **50**(11), 7020 (1979).
17. B.Z. Weiss, K.N.Tu, and D.A. Smith, *J. Appl. Phys.* 59(2), 415 (1986).
18. J.H. Buddery, A. J. Welch, *Nature* **167**, 362, (1951).
19. K. Schubert, S. Bhan, *Naturwiss* **47**, 303 (1960).
20. W. Jeitschko and E. Parthé, *Acta Cryst.* **22**, 417 (1967).
21. J. McCormack and J.-P. Fleurial in ***Modern Perspectives on Thermoelectrics and Related Materials***, edited by D.D. Allred, C.B. Vining and G.A. Slack, (Materials Research Society, Pittsburg, Pennsylvannia) 135 (1991).
22. W.L. Korst, L.N. Finnie, and A.W. Searcy, *J. Phys. Chem.* **61**, 1541 (1957).
23. L. Schellenberg, J.L. Jorda and J. Muller, *J. Less-Common Metals*, **109**, 261 (1985).